$Pb_2Cd(SeO_3)_2X_2$ (X = Cl, Br): Two Halogenated Selenites with Phase Matchable Second Harmonic Generation

Ya-Ping Gong, Chun-Li Hu, Yun-Xiang Ma, Jiang-Gao Mao, Fang Kong*

State Key Laboratory of Structural Chemistry, Fujian Institute of Research on the Structure of Matter, Chinese Academy of Sciences, Fuzhou 350002, P. R. China

E-mail: kongfang@fjirsm.ac.cn

Supporting Information

Figure S10. The refractive indices (n) and birefringence (Δn) of $Pb_2Cd(SeO_3)_2X_2$ (X=Cl, Br).

Computational Method

The single-crystal structural data of compounds $Pb_2Cd(SeO_3)_2X_2$ (X=Cl, Br) were used for the theoretical calculations. The electron structure calculations and optical properties were performed on the CASTEP code[1] in the Material Studio package, a total energy package based on plane-wave pseudopotential method using density functional theory (DFT). The generalized gradient approximation (GGA) of the Perdew-Burke-Ernzerhof (PBE) was used for the exchange-correlation energy[2]. The following valence-electron configurations were considered in the computation: Pb-$5d^{10}6s^26p^2$, Cd-$4d^{10}5s^2$, Se-$4s^24p^4$, O-$2s^22p^4$, Cl-$3s^23p^5$, Br-$4s^24p^5$. The numbers of plane waves include in the basis sets were determined by a cutoff energy of 820eV. The numerical integration of the Brillouin zone was performed using a Monkhorst-Pack *k*-point sampling of 5×4×1 and 4×4×1, respectively.

References

1 a) V. Milman, B. Winkler, J. A. White, C. J. Pickard, M. C. Payne, E. V. Akhmatskaya, R. H. Nobes, *Int. J. Quantum Chem.* 2000, **77**, 895-910; b) M. D. Segall, P. J. D. Lindan, M. J. Probert, C. J. Pickard, P. J. Hasnip, S. J. Clark, M. C. J. Payne, *Phys-Condens Mat.* 2002, **14**, 2717-2744.

2 a) J. P. Perdew, K. Burke, M. Ernzerhof, *Phys. Rev. Lett*. 1996, **77**, 3865-3868; b) S. J. Clark, M. D. Segall, C. J. Pickard, P. J. Hasnip, M. J. Probert, K. Refson, M. C. Payne, *Z. Kristallogr*. 2005, **220**, 567-570.

Table S1. Selected bond lengths (Å) for $Pb_2Cd(SeO_3)_2X_2$ (X=Cl, Br).

$Pb_2Cd(SeO_3)_2Cl_2$			
Pb(1)-O(1) #1	2.409(8)	Pb(1)-O(3)	2.694(9)
Pb(1)-O(1)	2.705(8)	Pb(1)-O(3)#2	2.715(8)
Pb(1)-Cl(2)#1	3.001(3)	Pb(1)-Cl(2)#3	3.077(3)
Pb(1)-Cl(1)#4	3.121(3)	Pb(1)-Cl(2)#2	3.156(3)
Pb(2)-O(6)#5	2.381(8)	Pb(2)-O(2)	2.460(8)
Pb(2)-O(4)#6	2.611(8)	Pb(2)-O(1)	2.643(9)
Pb(2)-O(3)#5	2.717(8)	Pb(2)-Cl(1)#4	3.131(3)
Cd(1)-O(2)	2.236(9)	Cd(1)-O(4)	2.305(8)
Cd(1)-O(4)#6	2.307(8)	Cd(1)-O(5)#5	2.330(7)
Cd(1)-O(5)#7	2.359(8)	Cd(1)-O(6)	2.626(8)
Cd(1)-Cl(1)#8	2.720(3)	Se(1)-O(1)	1.745(8)
Se(1)-O(2)	1.691(9)	Se(1)-O(3)	1.688(8)
Se(2)-O(4)	1.732(7)	Se(2)-O(5)	1.706(7)
Se(2)-O(6)	1.674(8)		
$Pb_2Cd(SeO_3)_2Br_2$			
Pb(1)-O(1)#1	2.434(8)	Pb(1)-O(1)	2.655(8)
Pb(1)-O(3)#2	2.689(8)	Pb(1)-O(3)	2.746(8)
Pb(1)-Br(2)#1	3.1353(13)	Pb(1)-Br(2)#3	3.1627(10)
Pb(1)-Br(2)#2	3.2038(14)	Pb(1)-Br(1)#4	3.2433(10)
Pb(2)-O(6)#5	2.408(7)	Pb(2)-O(2)	2.461(8)
Pb(2)-O(4)#6	2.591(7)	Pb(2)-O(1)	2.697(7)
Pb(2)-O(3)#5	2.751(8)	Pb(2)-Br(1)#4	3.2122(12)
Cd(1)-O(2)	2.255(8)	Cd(1)-O(4)#6	2.332(8)
Cd(1)-O(5)#5	2.348(8)	Cd(1)-O(4)	2.353(8)
Cd(1)-O(5)#7	2.423(8)	Cd(1)-O(6)	2.517(8)
Cd(1)-Br(1)#8	2.8337(12)	Se(1)-O(1)	1.730(8)
Se(1)-O(2)	1.689(8)	Se(1)-O(3)	1.699(8)
Se(2)-O(4)	1.734(7)	Se(2)-O(5)	1.697(7)
Se(2)-O(6)	1.677(8)		

Symmetry transformations used to generate equivalent atoms: For compound 1: #1 x+1/2, -y+3/2, -z+2 #2 x-1/2, -y+3/2, -z+2 #3 x, y-1, z #4 x, y, z #5 x-1, y, z #6 -x+1, y-1/2, -z+3/2 #7 -x+2, y-1/2, -z+3/2 #8 -x+1, y+1/2, -z+3/2. For compound 2: #1 x+1/2, -y+3/2, -z+2; #2 x-1/2, -y+3/2, -z+2; #3 x, y-1, z; #4 x, y, z; #5 x-1, y, z; #6 -x+1, y-1/2, -z+3/2; #7 -x+2, y-1/2, -z+3/2; #8 -x+1, y+1/2, -z+3/2.

Table S2. Atomic coordinates ($\times 10^4$) and equivalent isotropic displacement parameters ($A^2 \times 10^3$) for $Pb_2Cd(SeO_3)_2X_2$ (X=Cl, Br).

$Pb_2Cd(SeO_3)_2Cl_2$				
	x	y	z	U (eq)
Pb (1)	5084 (1)	5238 (1)	9798 (1)	12 (1)
Pb (2)	476 (1)	7111 (1)	8574 (1)	10 (1)
Cd (1)	5323 (1)	9498 (1)	9498 (1)	7 (1)
Se (1)	4944 (2)	9727 (1)	9162 (1)	7 (1)
Se (2)	9846 (2)	12240 (1)	7941 (1)	6 (1)
Cl (1)	4909 (5)	4328 (4)	8518 (1)	16 (1)
Cl (2)	4928 (5)	11469 (4)	10468 (1)	18 (1)
O (1)	2641 (13)	8421 (12)	9485 (4)	12 (2)
O (2)	4260 (14)	8950 (12)	8510 (4)	15 (2)
O (3)	7292 (13)	8342 (13)	9363 (4)	12 (2)
O (4)	7632 (12)	12169 (12)	7428 (3)	8 (2)
O (5)	12251 (12)	11754 (11)	7516 (3)	5 (2)
O (6)	9133 (13)	10157 (12)	8248 (4)	15 (2)
$Pb_2Cd(SeO_3)_2Br_2$				
	x	y	z	U (eq)
Pb (1)	4972 (1)	5343 (1)	9816 (1)	15 (1)
Pb (2)	433 (1)	7178 (1)	8557 (1)	14 (1)
Cd (1)	5328 (2)	9523 (1)	7645 (1)	10 (1)
Se (1)	4854 (2)	9730 (1)	9166 (1)	10 (1)
Se (2)	9830 (2)	12228 (1)	7915 (1)	8 (1)
Br (1)	4933 (2)	4336 (1)	8516 (1)	16 (1)
Br (2)	4902 (2)	11523 (1)	10492 (1)	18 (1)
O (1)	2629 (15)	8402 (10)	9479 (3)	14 (2)
O (2)	4173 (14)	9031 (9)	8521 (3)	15 (2)
O (3)	7256 (15)	8386 (11)	9348 (3)	17 (2)
O (4)	7629 (13)	12195 (11)	7411 (3)	9 (2)
O (5)	12234 (14)	11734 (11)	7511 (3)	12 (2)
O (6)	9042 (15)	10167 (11)	8205 (3)	19 (2)

Table S3. The state energies (eV) of the lowest conduction band (L-CB) and the highest valence band (H-VB) of $Pb_2Cd(SeO_3)_2X_2$ (X=Cl, Br).

Compounds	**k-point**	**L-CB**	**H-VB**
$Pb_2Cd(SeO_3)_2Cl_2$	G (0.000, 0.000, 0.000)	3.68045	-0.14708
	Z (0.000, 0.000, 0.500)	3.66716	-0.18124
	T (-0.500, 0.000, 0.500)	3.75460	-0.23169
	Y (-0.500, 0.000, 0.000)	3.73588	-0.22838
	S (-0.500, 0.500, 0.000)	3.95448	-0.08060
	X (0.000, 0.500, 0.000)	3.88604	-0.04936
	U (0.000, 0.500, 0.500)	3.88217	-0.05854
	R (-0.500, 0.500, 0.500)	3.97239	-0.08806
$Pb_2Cd(SeO_3)_2Br_2$	G (0.000, 0.000, 0.000)	3.42520	-0.25561
	Z (0.000, 0.000, 0.500)	3.41453	-0.26799
	T (-0.500, 0.000, 0.500)	3.55638	-0.14225
	Y (-0.500, 0.000, 0.000)	3.53919	-0.15050
	S (-0.500, 0.500, 0.000)	3.80459	-0.07441
	X (0.000, 0.500, 0.000)	3.54964	-0.03454
	U (0.000, 0.500, 0.500)	3.54626	-0.04387
	R (-0.005, 0.500, 0.500)	3.82870	-0.07901

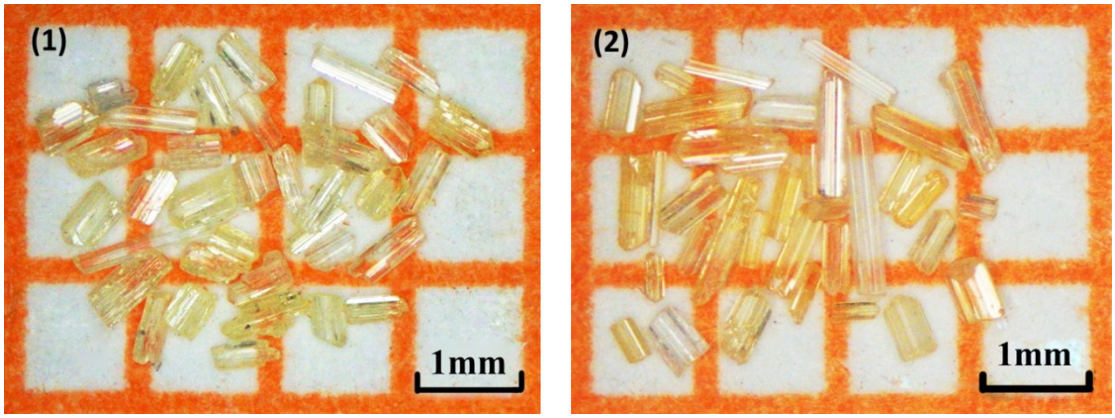

Figure S1. As-grown crystals of compounds $Pb_2Cd(SeO_3)_2Cl_2$ (1) and $Pb_2Cd(SeO_3)_2Br_2$ (2) .

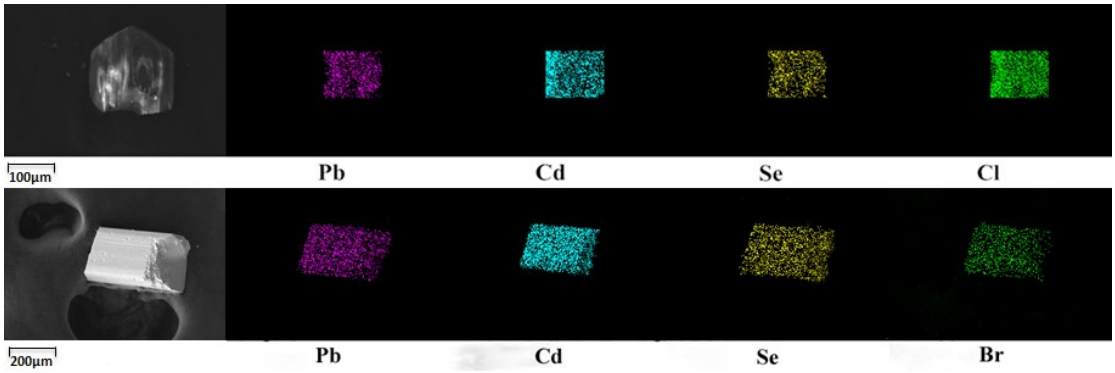

Figure S2. SEM images of compounds $Pb_2Cd(SeO_3)_2X_2$ (X=Cl, Br) and their elemental distribution maps.

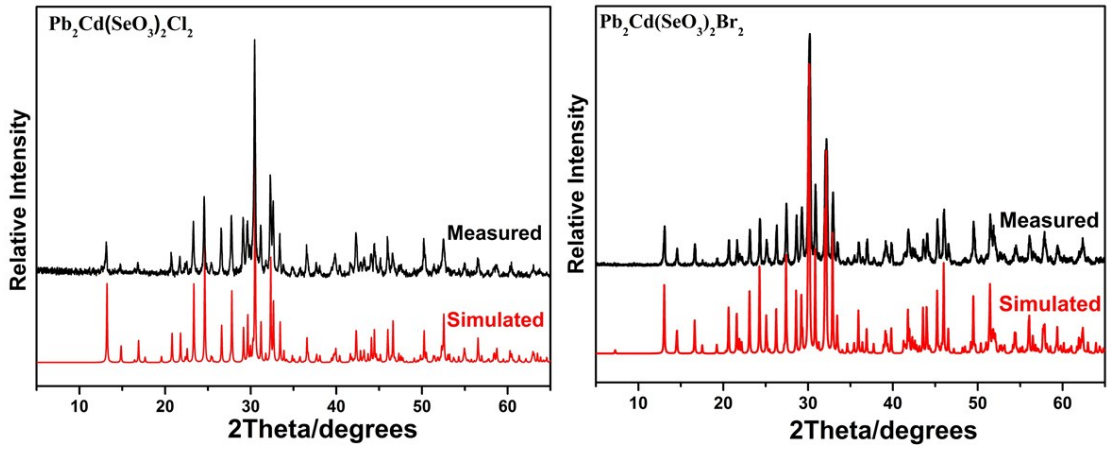

Figure S3. Simulated and measured powder X-ray diffraction patterns of $Pb_2Cd(SeO_3)_2X_2$ (X=Cl, Br).

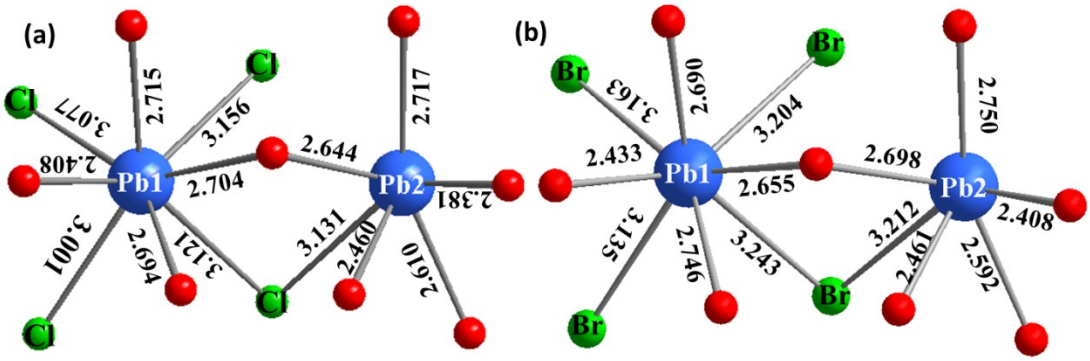

Figure S4. The coordination environments of Pb(1) and Pb(2) in $Pb_2Cd(SeO_3)_2Cl_2$ (a) and $Pb_2Cd(SeO_3)_2Br_2$ (b).

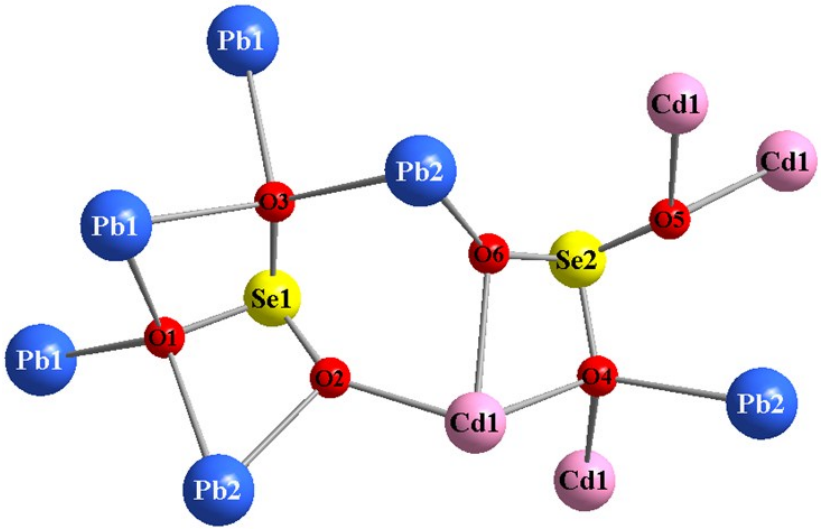

Figure S5. The coordination environments of $Se(1)O_3$ and $Se(2)O_3$ groups in $Pb_2Cd(SeO_3)_2X_2$ (X=Cl, Br).

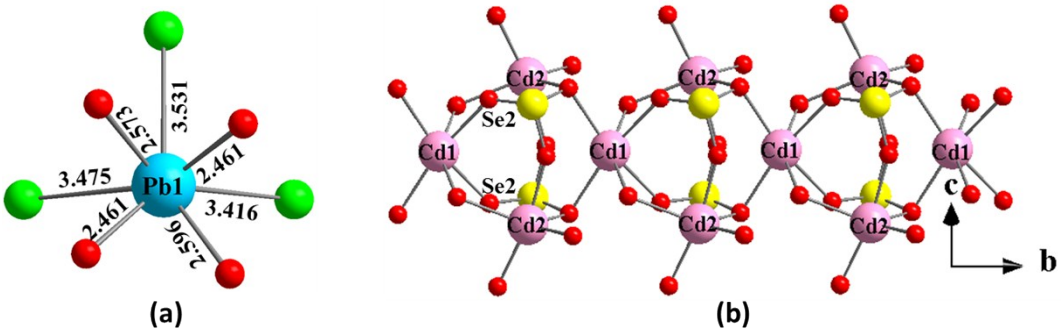

Figure S6. The coordination environments of Pb(1) (a) and the 1D cadmium selenite chain in $Pb_2Cd_3(SeO_3)_4I_2(H_2O)$ (b).

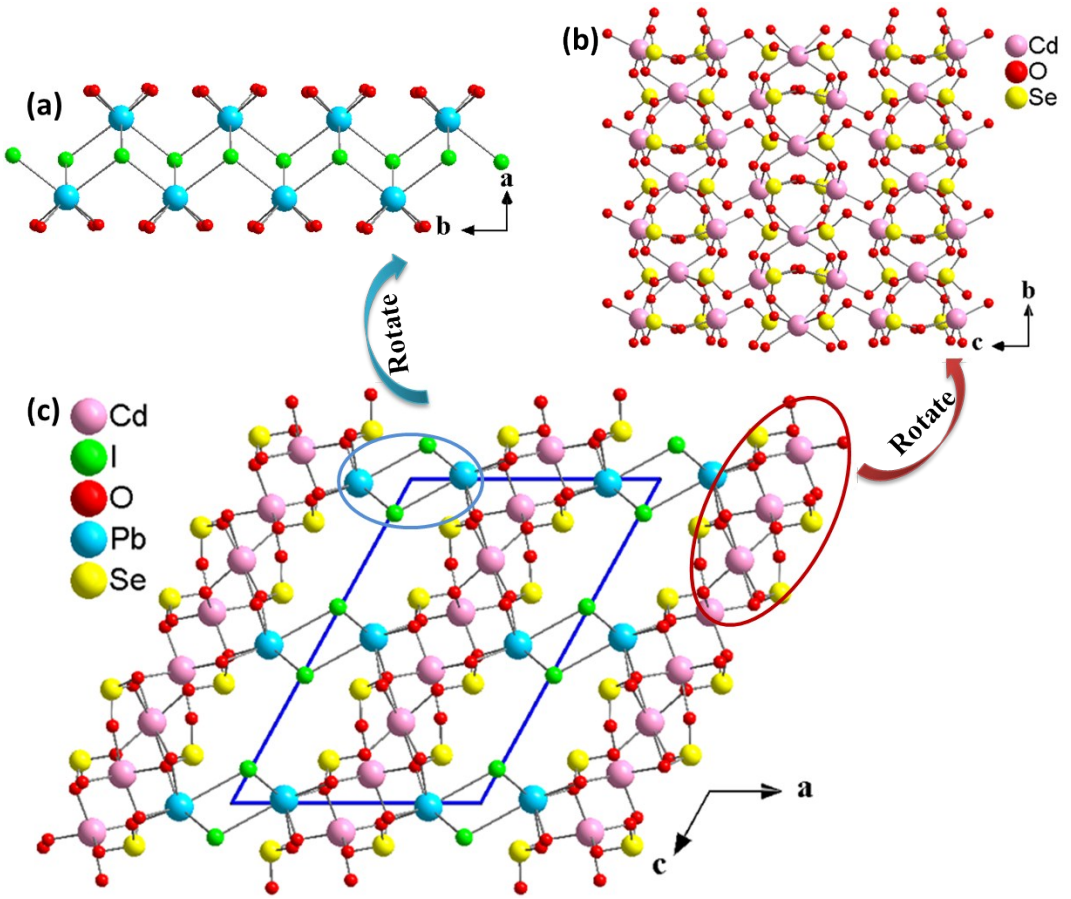

Figure S7. The 1D $[PbO_4I_3]_n$ chain (a), the 2D cadmium selenite layer along *a*-axis (b) and the 3D framework of $Pb_2Cd_3(SeO_3)_4I_2(H_2O)$ (c) along *b*-axis.

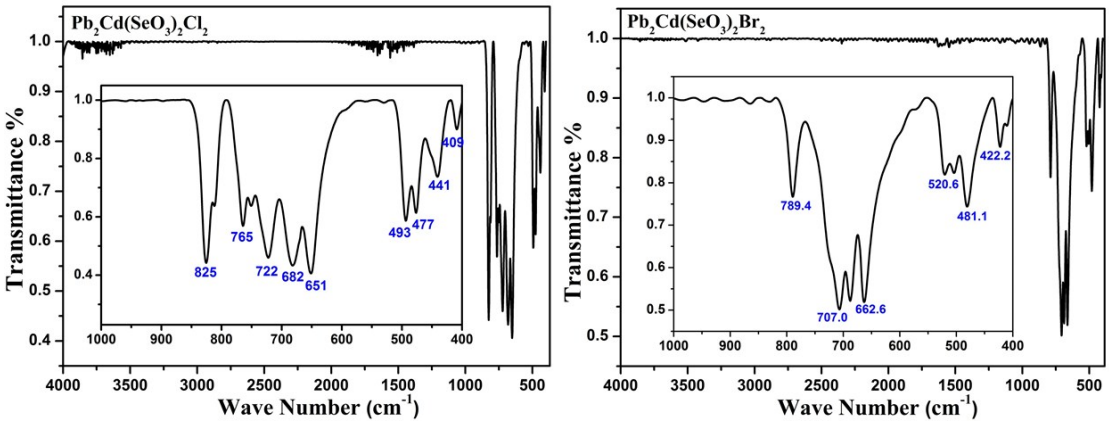

Figure S8. IR spectra of compounds $Pb_2Cd(SeO_3)_2X_2$ (X=Cl, Br).

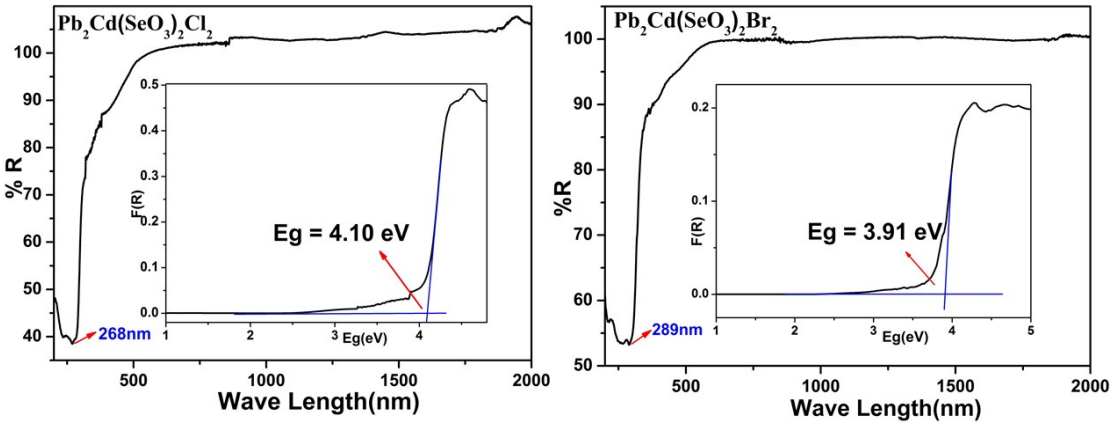

Figure S9. UV-vis-NIR spectra of compounds $Pb_2Cd(SeO_3)_2X_2$ (X=Cl, Br).

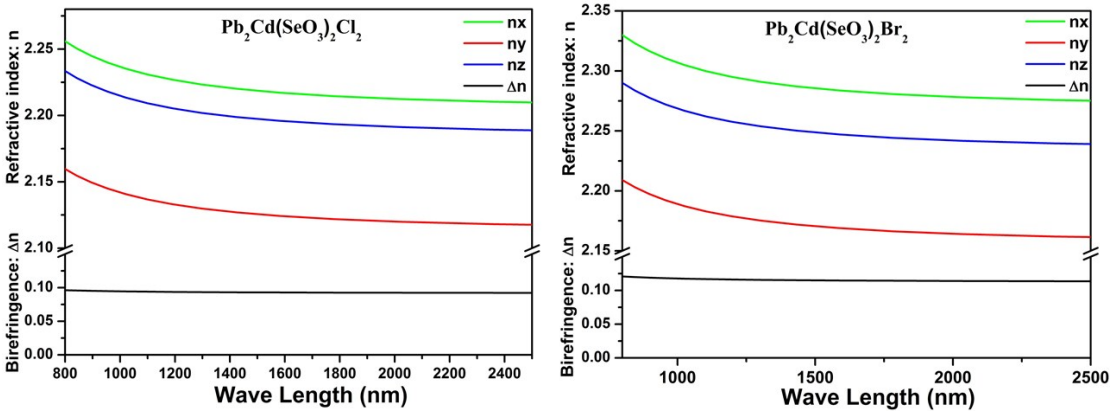

Figure S10. The refractive indices (n) and birefringence (Δn) of $Pb_2Cd(SeO_3)_2X_2$ (X=Cl, Br).